JOURNAL OF MATERIALS SCIENCE 21 (1986) 744–750

Hierarchical structure in a thermotropic liquid-crystalline copolyester

T. WENG, A. HILTNER, E. BAER
Department of Macromolecular Science, Case Institute of Technology, Case Western Reserve University, Cleveland, Ohio 44106, USA

Thermotropic liquid-crystalline polyesters are a new class of polymeric materials which have unique molecular and solid-state structures, flow characteristics and mechanical properties. Injection-moulded plaques were found to consist mainly of three highly anisotropic, flow-induced macrolayers: two skins with a core in between. By using fractographic methods, the internal solid-state structure of the macrolayers was elucidated. A hierarchical structure has been proposed describing the observed levels of organization. The skin macrolayer has a distinct structural gradient comprised of three subdivisions from the surface inward: a highly oriented top layer, several oriented sublayers and a less oriented inner zone. The top layer is fibrillar in nature and the sublayers consist of stacks of interconnected microlayers. In the core, no well-defined substructure was observed, yet molecular orientation perpendicular to the injection direction represented the localized flow patterns.

1. Introduction

Liquid-crystalline substances have been known for almost a century. The materials are characterized as having structures intermediate between isotropic fluids and three-dimensional ordered crystals. Their classification and properties are well documented in the literature [1, 2]. Polymeric systems exhibiting liquid-crystalline behaviour, on the other hand, were observed more recently mainly in lyotropic biopolymers [3]. Flory [4] as well as others [5, 6] predicted theoretically the formation of liquid-crystalline phases in polymers based on phase separation in concentrated solutions of rigid rodlike macromolecules. Due to molecular order in solution or in the melt, liquid-crystalline main chain polymers can by proper processing be highly chain-extended, and as a result very high moduli can be obtained. About twenty years ago, the anisotropic behaviour of aromatic polyamides in solution was discovered [7], and the potential importance of liquid-crystalline polymers in the area of high performance fibres was realized which led to the development of Kevlar aramid fibres. Jackson and Kuhfus [8] subsequently reported an aromatic–aliphatic copolyester which exhibited liquid-crystalline behaviour in the melt. Following these two major developments, the extensive amount of industrial and academic research carried out in recent years is leading to the birth of a new class of polymeric materials unique both in molecular structure and mechanical properties [9, 10].

This paper is concerned with thermotropic liquid-crystalline polymers from aromatic polyesters. Contrary to the lyotropic types which exhibit a liquid-crystalline phase in solution [11], the thermotropics can be processed directly from the melt by conventional methods such as melt-spinning, extrusion and injection-moulding. Since these aromatic polyesters have high melting ranges, a number of routes have been proposed to reduce the melting points to within a range suitable for processing while still maintaining the necessary chain stiffness [12]. The introduction of flexible units [13], kinks and bends [14], unsubstituted aromatic modifiers along the chain [15], and random copolymerization [16] were amongst the approaches used.

Most of the early research activities were concentrated on exploring the synthesis and chemical structure of these polymers. Although a number of investigators have studied the solid-state structure of the copolyester used in this work [17–20], relatively little has been reported on characterizing the process-induced solid-state morphology. Ophir and Ide [21] observed the presence of a layer-like structure resulting from complex flows during mould filling. Similarly, Thapar and Bevis [22] reported sheet-like structures from etched surfaces viewed in the scanning electron microscope (SEM).

The purpose of this study was to elucidate the hierarchical morphological structure that resulted from the complex flow patterns produced in injection-moulded parts. It should be noted that similar hierarchical structures have also been observed in fibres made from this type of thermotropic polymer [23] as well as in Kevlar fibres [24]. In order to enhance our understanding of the physical and mechanical properties of these polymers a more comprehensive understanding of their solid-state structure is warranted.

2. Experimental details

2.1. Material

The material used in this study was a copolyester consisting of 58 mol % *p*-hydroxybenzonic acid (HBA) and 42 mol % 6,2-hydroxynaphthoic acid

0022–2461/86 $03.00 + .12

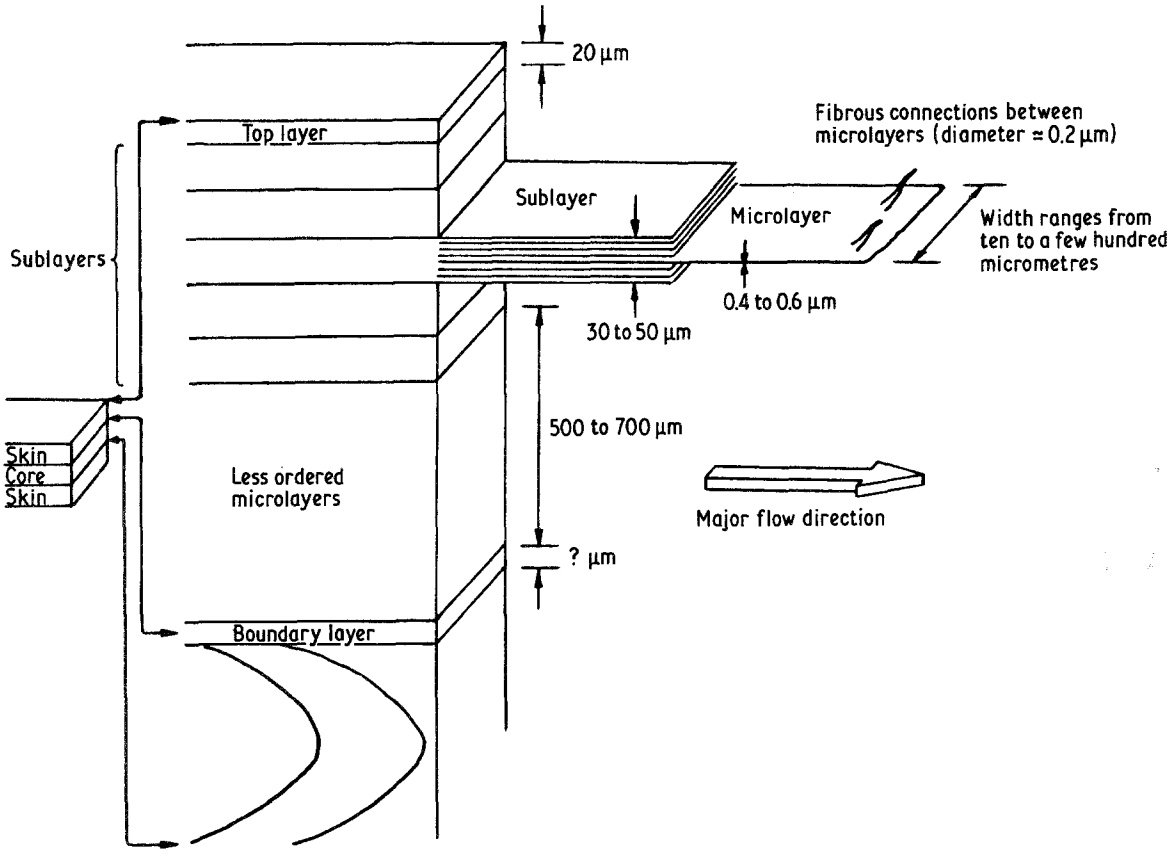

Figure 1 Schematic illustration of the proposed hierarchical model (not drawn to scale).

(HNA). The copolymer was generously supplied by the Celanese Research Corporation, Summit, New Jersey, in the form of injection-moulded plaques having the dimensions 8 in. × 2 in. × 1/8 in. (203 mm × 51 mm × 3 mm). The moulding conditions were as follows: melt temperature 263° C, mould temperature 63° C and injection pressure 20 000/5000 psi (138/35 MPa).

2.2. Scanning electron microscopy

To study the fracture surfaces, the SEM used was a Cambridge Stereo Scan Type S4–10. Samples were coated with palladium prior to examination at magnifications between 20× and 10 000×.

2.3. Wide-angle X-ray measurements

X-ray diffraction patterns were obtained with a Searle toroidal focusing camera and nickel-filtered Cu$K\alpha$ radiation. Samples from the skin macrolayer were obtained by sectioning the skin with a diamond wafering blade in an Isomet apparatus. Slices ranged between 70 and 330 μm in thickness. Samples from the core macrolayer were obtained by milling away both surfaces by means of a fly-type cutter in a milling machine until the required thickness of about 1 mm was achieved.

3. Results and discussion

3.1. Hierarchical model

SEM micrographs and the visual appearance of the fracture surfaces revealed the presence of a complex hierarchical organization. Based on observations of morphological substructures, a descriptive model given in Fig. 1 is proposed. This model can serve as the basis for understanding the mechanical behaviour.

Starting from the macroscopic level, three macrolayers were observed: two skins with a core in between, each representing approximately one-third of the total thickness. Due to differences in colour, the macrolayers are readily visible to the naked eye. This skin-core morphology which is a characteristic of many injection-moulded polymers [25–28], is clearly demonstrated in Fig. 2. A typical fracture surface of a specimen broken in tension and pulled at 90° to the flow direction is shown. The draw direction is normal to the plane of the picture, while the flow direction is vertical in the micrograph. The orientation of each macrolayer is different, and the skin seems to be

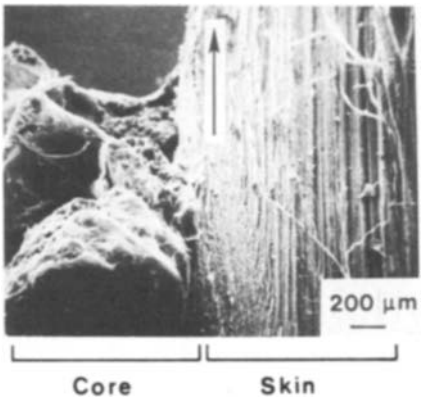

Figure 2 Scanning electron micrograph of a typical fracture surface of a specimen broken in tension, showing the skin and core macrolayers. The flow direction is indicated by the arrow and the pulling direction is normal to the plane of the picture.

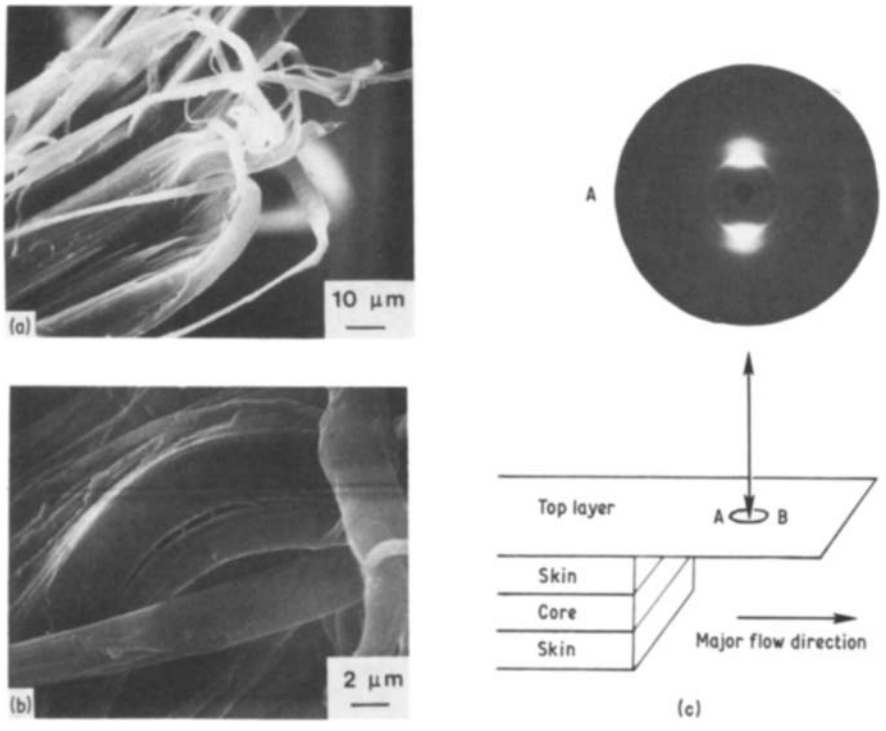

Figure 3 (a) Scanning electron micrograph of a portion of the top layer of the skin after being pulled parallel to the flow direction. (b) Magnification of the centre of micrograph (a). (c) WAXS of the top layer, showing the high degree of orientation parallel to the major flow direction.

oriented parallel to the flow direction while the core is oriented perpendicular to the flow.

Up to four distinct macrolayers have been reported in another thermotropic copolyester [21]. The macrolayers were examined in polished cross-sections of moulded tensile bars between crossed polars in an optical microscope. Although the thickness of the observed layers was reported to be highly dependent on the moulding conditions (specifically the flow cross-section), no microstuctural or morphological details of the layers were given.

3.2. Skin macrolayer

By proceeding to higher magnifications, the next level of organization as illustrated in the model (Fig. 1) was shown to be composite in itself. This composite was composed of structures which changed as one proceeded from the surface inward, thus giving a gradient of morphologies.

3.2.1. Top layer

This thin layer, approximately 20 μm in thickness, is responsible for the shiny texture of the surface. As indicated in Fig. 3a, this layer is fibrous in nature and is oriented parallel to the flow direction. Fig.3b, a magnification taken from the centre of Fig. 3a, emphasizes the fibrillar nature. From the wide-angle X-ray scattering (WAXS) shown in Fig. 3c, the high degree of molecular orientation in this thin layer parallel to the injection direction is confirmed.

3.2.2. Sublayers

Fig. 4a, which is a magnification of the right-hand side of Fig. 2, shows many subdivisions under the top layer. They are essentially parallel to the flow direction and range somewhere between 30 and 50 μm in thickness. The average molecular orientation within the sublayers is also parallel to the flow, as seen in the WAXS of Fig. 4b. The high orientation observed could be attributed to the elongational flows which seem to predominate near the surface of the mould [29, 30]. Closer examination of the sublayer in Figs. 5a and b shows stacks of many smaller subunits which appear to be microlayers of about 0.5 μm in thickness. These microlayers seem to be the smallest unit which we could observe with these methods, and are the third level of organization after the macrolayers and sublayers. These levels of organization, which are shown again in fracture surfaces taken from samples deformed in the flow direction (Figs. 6a and b), indicate a "mica-like" structure.

So far, the previous micrographs did not disclose

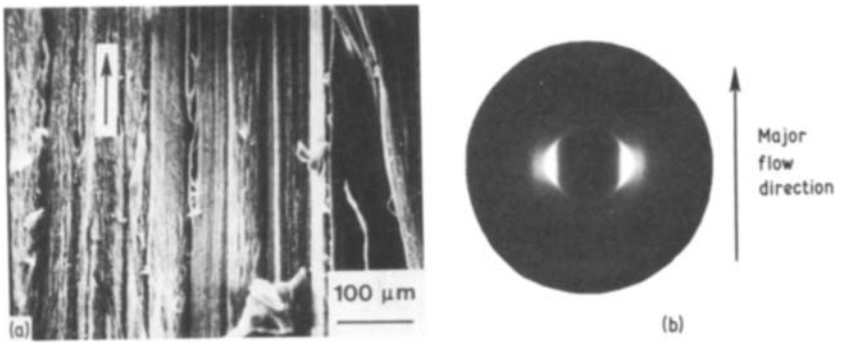

Figure 4 (a) Scanning electron micrograph of a fracture surface of the skin, showing the sublayers. The pulling direction is perpendicular to the plane of the micrograph and to the major flow direction which is indicated by the arrow. (b) The corresponding WAXS of the sublayers, showing molecular orientation parallel with the major flow direction.

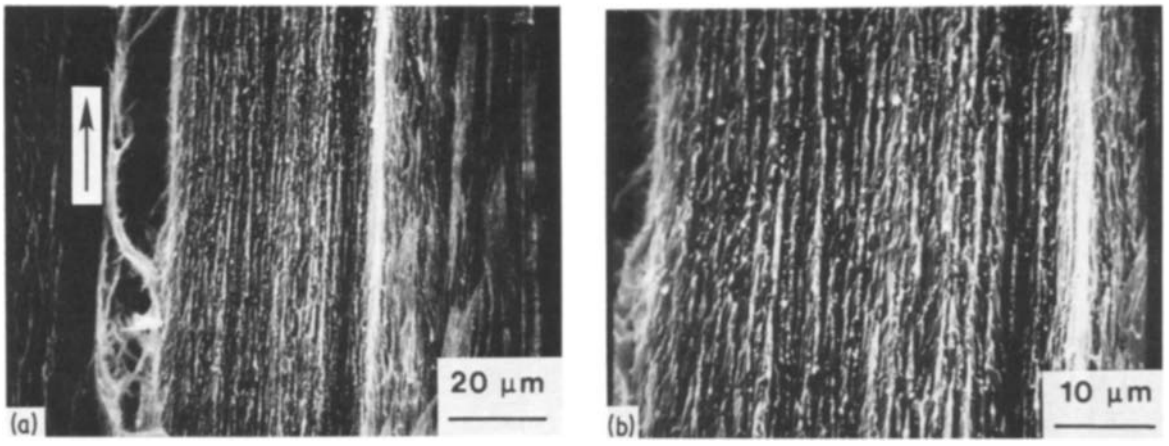

Figure 5 Scanning electron micrographs of a fracture surface of the skin showing (a) a sublayer and (b) stacks of microlayers. The flow direction is indicated by the arrow.

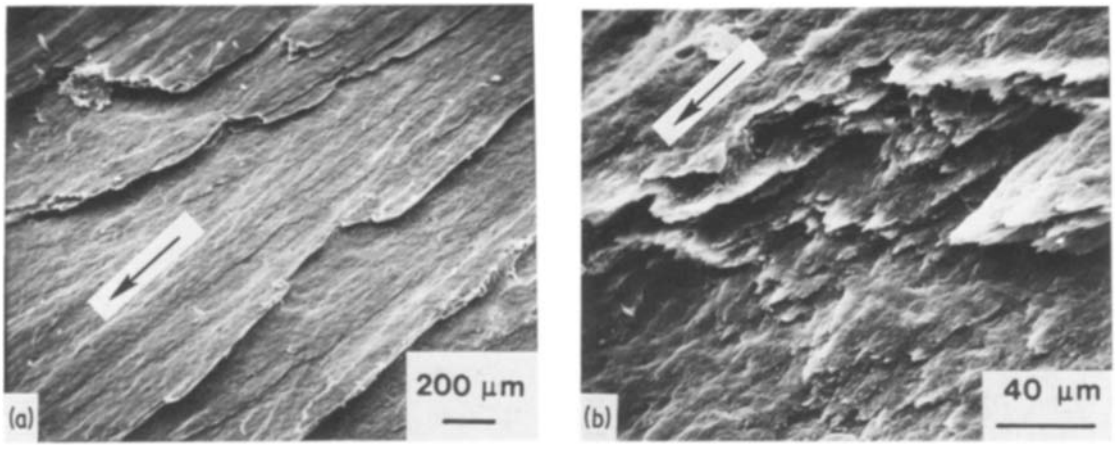

Figure 6 Scanning electron micrographs of a fracture surface of the skin showing (a) the "mica-like" structure of the sublayers and (b) the microlayers after being pulled parallel to the flow direction which is indicated by the arrow.

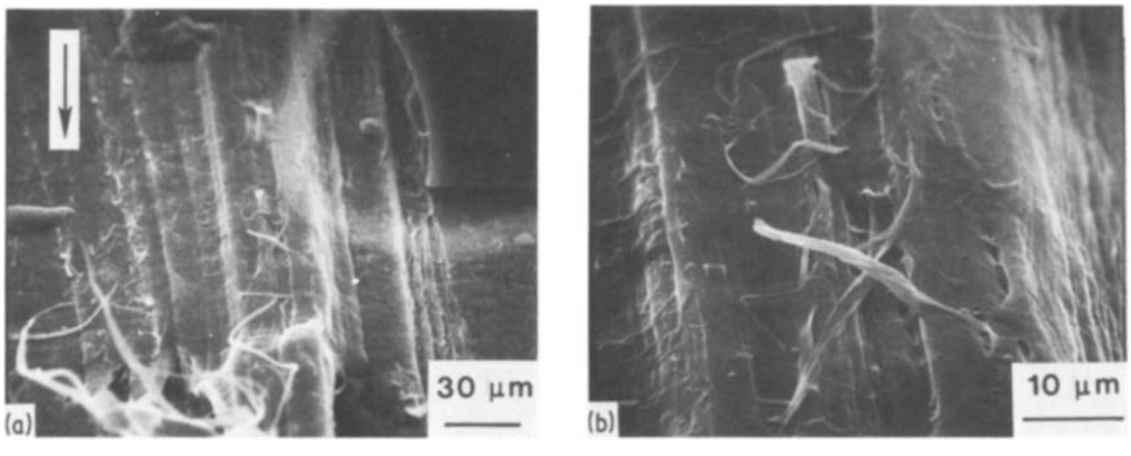

Figure 7 Scanning electron micrographs of a fracture surface of the skin revealing possible lateral dimensions of the microlayers. (b) is a magnification of the centre of (a). Flow and pulling directions are parallel and are indicated by the arrow.

any information on the lateral dimensions of the microlayers. Observations in Figs. 7 and 8 suggest that the width of the microlayers is in the range of 10 to 30 μm, and subsequently, the microlayers are better described as strips. A closer look at the strips (Fig. 7b) shows that they can be dissociated into fibres of only a few micrometres in width. However, in some micrographs the microlayers were found to reach up to hundreds of micrometres in width, and the question as to whether the strips are induced by deformation remains unresolved.

3.2.3. Less ordered microlayers

Sublayers are comprised of numerous microlayers, as illustrated in the hierarchical model of Fig. 1. Observations inside the skin away from the top layer show

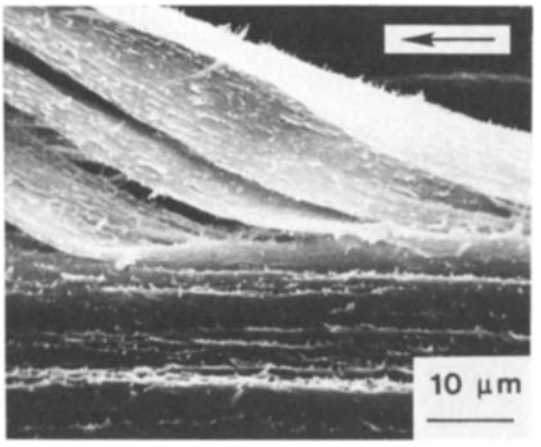

Figure 8 Scanning electron micrograph of a fracture surface of the skin, revealing the possible lateral dimensions of the microlayers (upper part). The major flow direction is shown by the arrow.

only the "basic unit" of the skin, the microlayers. However, these microlayers are far less ordered, are thicker and have a more fibrous character than the microlayers seen in the sublayers nearer to the surface (Fig. 9a). The microla.ers seem to disintegrate into numerous fibrillar segments as a result of intense irreversible deformation at the interfacial regions within the bulk structure. Other investigators [22] have observed sheets composed of nodulated fibrils ranging from 0.1 to 0.3 μm in diameter. The sheets were found also to increase in thickness through the section towards the core. Although their thicknesses (3 to 5 μm) are slightly greater than those of the microlayers (0.5 to 2 μm), the diameters of the fibrils seem to be of the same order of magnitude as the fibrillar segments shown in Fig. 9a. It is possible that other levels of organization between 500 nm and the molecular level [31] exist which were beyond the scope of this study. Again, the average molecular orientation of these less ordered microlayers is still parallel to the flow direction as seen from the WAXS in Fig. 9b, though the pattern shows less orientation than those shown in Figs. 3c and 4b. This zone within the so-called skin layer stretched from 500 to 700 μm in thickness, and might even include a boundary or transition zone that separates the skin from the core macrolayer. At present, little information is available about this boundary zone. At this point, it must be re-emphasized that our observations obviously show a hierarchical structure within the entire skin zone. However, this structural gradient changes in a systematic manner from the surface inwards and is strongly controlled by both the flow patterns in sample formation and the quench kinetics.

3.2.4. Microlayers interactions

Two techniques were employed to investigate the nature of the structural interconnections that hold the microlayers together. In the first method, the skin macrolayer was fractured at liquid nitrogen temperature in a plane parallel to the layers and to the flow direction by using a razor blade. The fracture surface obtained is shown in Fig. 10a. Torn, non-uniform fibres, believed to be the interconnections, are easily identified. Their widths range between 1 and 10 μm (Fig. 10b) and can reach up to 25 to 30 μm as seen in Fig. 10a. This is the common width of the strips discussed earlier. To emphasize the density and scale of these interconnections another micrograph is given in Fig. 11.

In the second method, the skin macrolayer was drawn normal to the flow in the vertical direction, that is in the thickness direction. Fig. 12a shows pulled microlayers 0.5 μm in thickness similar to those in Fig. 5. Between the microlayers (Fig. 12b) very thin fibrous interconnections 0.2 to 0.3 μm in diameter are clearly observed.

3.3. Core macrolayer

This macrolayer represents the remaining third of the plaque which is sandwiched between the two skin macrolayers. No structural hierarchical organization as exhibited by the skin macrolayer could be detected from studies of the fracture surface. Tightly packed flow lines (Fig. 13) representing the flow pattern of the injection moulding are visible to the naked eye in the centre plane of the core macrolayer. The core was obtained by milling away the skin macrolayers by means of a fly-type cutter in a milling machine. When viewed from the longitudinal cross-section along the centre line, these packed lines or bands take the shape of parabolaes headed in the direction of flow. Presumably plug flow, which predominates throughout the centre part of the plaque, gives rise to these parabolic curves.

From WAXS data taken at several points along the lines of flow (Fig. 14) the preferred molecular orientation was found to be parallel to the pattern lines. It can therefore, be concluded that the flow pattern represents the molecular orientation in the core macrolayer.

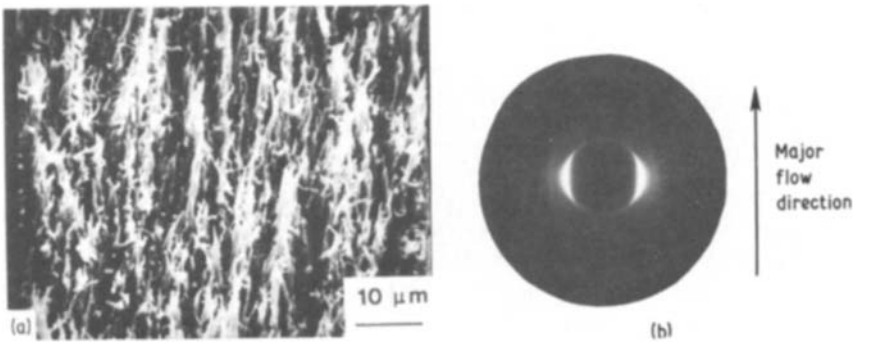

Figure 9 (a) Scanning electron micrograph of a fracture surface of the skin showing less ordered, more fibrillate microlayers zone. (b) The corresponding WAXS of this microlayers zone.

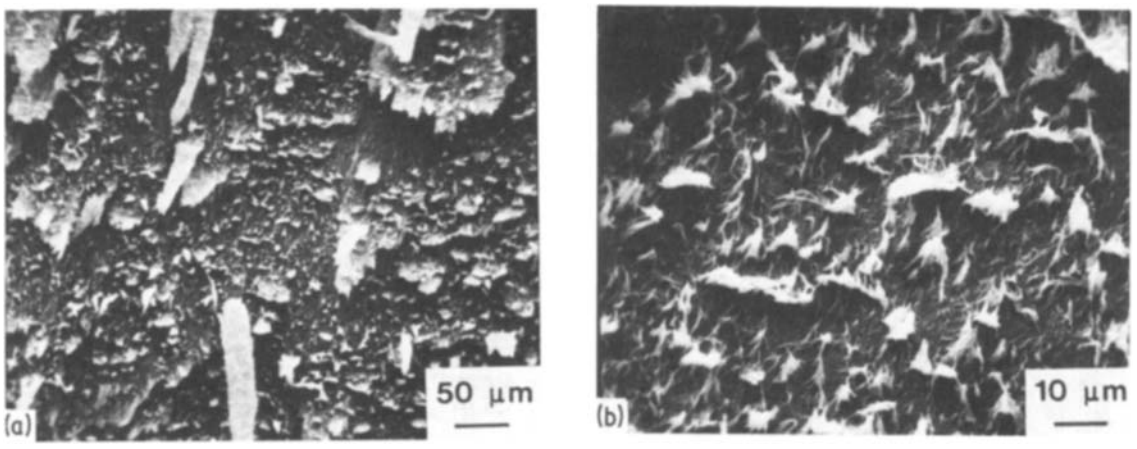

Figure 10 (a) Scanning electron micrograph of a fracture surface of the skin after being chopped parallel to the flow direction at liquid nitrogen temperature. (b) Magnification of the centre of (a).

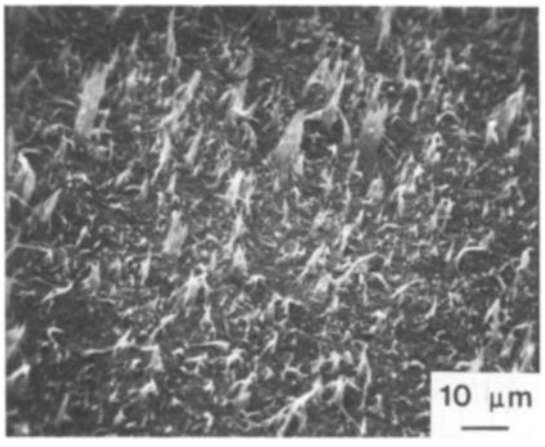

Figure 11 Scanning electron micrograph of a chopped skin layer at liquid nitrogen temperature, showing many fibrous connections.

The transverse orientation along the centre line of the plaque (Fig. 13) has been reported for other injection-moulded systems such as short glass-fibre-filled epoxy compounds [32] and polypropylene [33]. It was found that fan-type gates, characterized by a divergence section at the entrance of the mould, always lead to transverse orientation that is highly dependent on the filling rate. Deceleration at the gate creates compressive forces along the flow direction which cause the short fibres to rotate 90° to the flow. At high filling rates, plug flow occurs. Subsequently, the fibre orientation in the final moulding is similar to the transverse orientation as induced at the gate. It seems that a successful analysis for the flow processes during mould filling of these polymers can be achieved by using flow concepts applicable to short-fibre reinforced composites [29, 34].

4. Conclusion

Injection-moulded thermotropic liquid-crystalline copolyesters have a highly anisotropic "skin–core" structure. Based on the SEM micrographs of fracture surfaces, a hierarchical organization of layers of several levels has been proposed. The skin macrolayer was shown to consist of three subdivisions: a highly oriented top layer, several oriented sublayers and a less oriented inner zone. The distribution of molecular orientation in the core, which did not exhibit any hierarchical structures, was found to be represented by the localized flow pattern. The gradient of structure could be directly related to the flow characteristics of a molecular composite reminiscent of short-fibre reinforced systems.

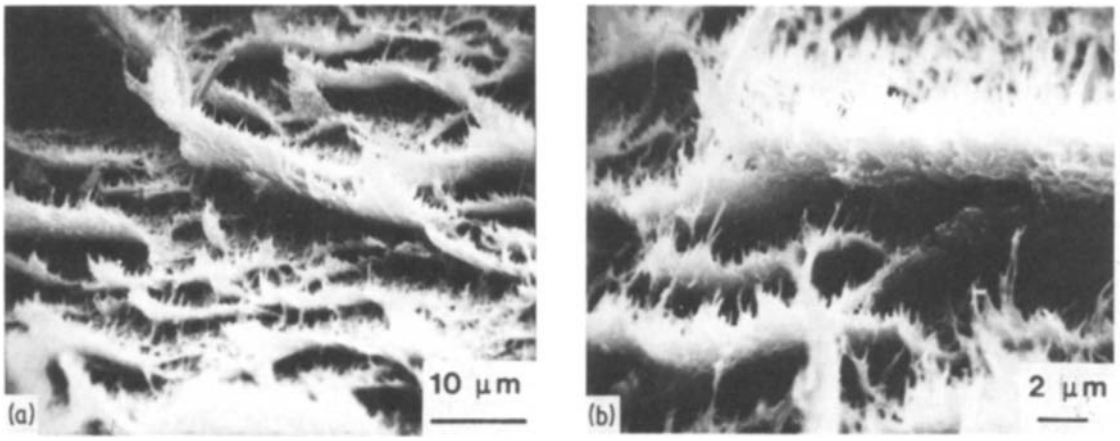

Figure 12 (a) Scanning electron micrograph of a fracture surface of the skin showing microlayers pulled apart in the vertical direction, i.e. in the thickness direction. (b) Magnification of the centre of (a) showing the fibrous interconnections.

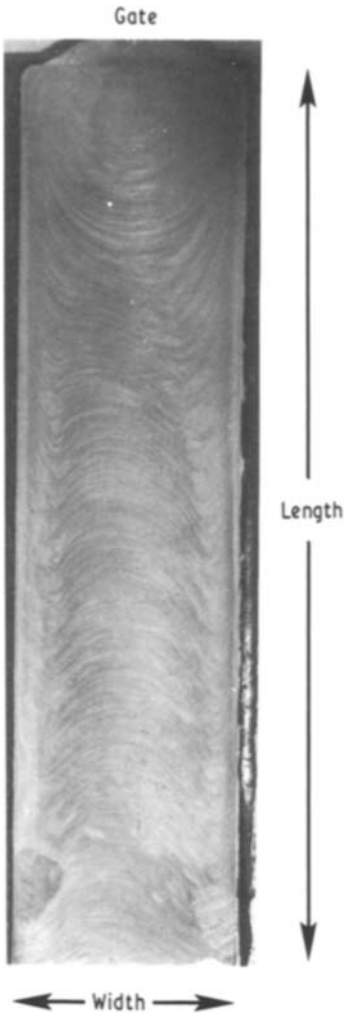

Figure 13 Photograph of the final flow pattern obtained in the moulded plaque.

Acknowledgements

The authors wish to thank Drs M. Jaffe, S. Grag and R. Chivers for helpful discussions. This work received generous financial support from the Celanese Company and the National Science Foundation (grant ISI 81–16103) through their co-sponsorship of the Center for Applied Polymer Research at Case Western Reserve University.

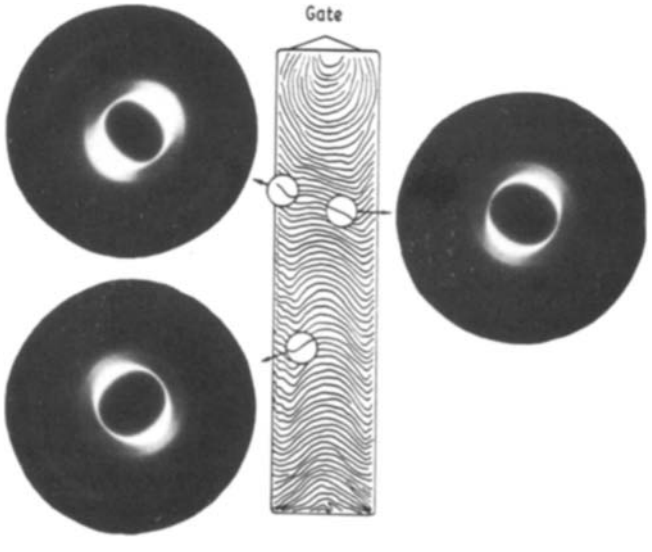

Figure 14 Schematic illustration of the pattern of flow, showing molecular orientation parallel with the lines of flow as demonstrated from the WAXS taken at different points.

References

1. G. W. GRAY and P. E. WINSOR (editors), "Liquid Crystals and Plastic Crystals" (Wiley, New York, 1974).
2. P. E. DE GENNES, "The Physics of Liquid Crystals" (Oxford University Press, Oxford, 1979).
3. F. C. BAWDEN and N. W. PIRIE, *Proc. R. Soc.* **B123** (1937) 274.
4. P. J. FLORY, *ibid.* **A234** (1956) 73.
5. L. ONSAGER, *Ann. N. Y. Acad. Sci.* **51** (1949) 627.
6. A. ISHIHARA, *J. Chem. Phys.* **19** (1951) 1142.
7. S. L. KOWLEK, US Patent No. 3 600 350 (1971).
8. W. J. JACKSON and H. F. KUHFUSS, *J. Polym. Sci. Polym. Chem. Ed.* **14** (1976) 2043.
9. E. T. SAMUKSLI and D. B. DUPRE, "Advances in Liquid Crystals", Vol. 4, edited by G. H. Brown (Academic Press, New York, 1979).
10. A. BLUMSTEIN, "Liquid Crystalline Order in Polymers" (Academic Press, New York, 1978).
11. P. W. MORGAN, *Macromol.* **10** (1977) 1381.
12. W. J. JACKSON, *Brit. Polym. J.* **12** (1980) 154.
13. W. J. JACKSON and H. F. KUHFUSS, US Patent No. 4 140 846 (1979).
14. W. J. JACKSON and J. C. MORRIS, US Patent No. 4 181 792 (1980).
15. G. CALUNDANN, US Patent No. 4 067 852 (1978).
16. S. G. COTTIS, J. ECONOMY and B. E. NOWAK, US Patent No. 3 637 595 (1972).
17. C. VINEY, A. M. DONALD and A. H. WINDLE, *J. Mater. Sci.* **18** (1983) 1136.
18. A. M. DONALD and A. H. WINDLE, *ibid.* **18** (1983) 1143.
19. D. J. BLUNDELL, *Polymer* **23** (1982) 359.
20. G. A. GUTIERREZ, R. A. CHIVERS, J. BLACKWELL, J. B. STAMATOFF and H. YOON, *ibid.* **24** (1983) 937.
21. Z. OPHIR and Y. IDE, *Polym. Eng. Sci.* **23** (1983) 792.
22. H. THAPAR and M. BEVIS, *J. Mater. Sci. Lett.* **2** (1983) 733.
23. M. JAFFE, private communication (1984).
24. L. S. LI, L. F. ALLARD and W. C. BIGELOW, *J. Macromol. Sci. (Phys.)* **B22**(2) (1983) 269.
25. E. S. CLARK, *Soc. Plast. Eng. J.* **23** (1967) 46.
26. J. E. CALLEAR and J. B. SHORTALL, *J. Mater. Sci.* **12** (1977) 141.
27. M. R. KANTZ, H. D. NEWMAN and F. H. STIGALE, *J. Appl. Polym. Sci.* **16** (1972) 1249.
28. V. TAN and M. KAMAL, *ibid.* **22** (1978) 2341.
29. Y. IDE and Z. OPHIR, *Polym. Eng. Sci.* **23** (1983) 261.
30. D. G. BAIRD and G. L. WILKES, *ibid.* **23** (1983) 632.
31. R. A. CHIVERS, J. BLACKWELL and G. A. GUTIERREZ, *Polymer* **25** (1984) 435.
32. L. A. GOETTLER, *Mod. Plast.* **47** (1970) 140.
33. P. F. BRIGHT, R. J. CROWSON and M. J. FOLKES, *J. Mater. Sci.* **13** (1978) 2497.
34. K. F. WISSBURN, *J. Rheol.* **23** (1981) 619.

Received 16 October 1984
and accepted 29 March 1985